Alternative N-Terminal Regions of *Drosophila* Myosin Heavy Chain Tune Muscle Kinetics for Optimal Power Output

Douglas M. Swank,* William A. Kronert,[†] Sanford I. Bernstein,[†] and David W. Maughan*

*Department of Molecular Physiology and Biophysics, University of Vermont, Burlington, Vermont 05405; and
[†]Biology Department and Molecular Biology Institute, San Diego State University, San Diego, California 92182-4614

ABSTRACT   We assessed the influence of alternative versions of a region near the N-terminus of *Drosophila* myosin heavy chain on muscle mechanical properties. Previously, we exchanged N-terminal regions (encoded by alternative exon 3s) between an embryonic (EMB) isoform and the indirect flight muscle isoform (IFI) of myosin, and demonstrated that it influences solution ATPase rates and in vitro actin sliding velocity. Because each myosin is expressed in *Drosophila* indirect flight muscle, in the absence of other myosin isoforms, this allows for muscle mechanical and whole organism locomotion assays. We found that exchanging the flight muscle specific exon 3 region into the embryonic isoform (EMB-3b) increased maximum power generation (P_{max}) and optimal frequency of power generation (f_{max}) threefold and twofold compared to fibers expressing EMB, whereas exchanging the embryonic exon 3 region into the flight muscle isoform (IFI-3a) decreased P_{max} and f_{max} to ~80% of IFI fiber values. *Drosophila* expressing IFI-3a exhibited a reduced wing beat frequency compared to flies expressing IFI, which optimized power generation from their kinetically slowed flight muscle. However, the slower wing beat frequency resulted in a substantial loss of aerodynamic power as manifest in decreased flight performance of IFI-3a compared to IFI. Thus the N-terminal region is important in tuning myosin kinetics to match muscle speed for optimal locomotory performance.

INTRODUCTION

The functional diversity of striated muscle is due in large part to different isoforms of myosin, which enable specialized muscle fiber types to respond to different locomotory demands. Myosin isoforms are the primary determinants of shortening velocity or optimal muscle operational frequency, force, and power-generating ability (Lowey et al., 1993). Sequence comparisons and in vitro functional studies at the molecular level suggest that specific structural domains of the myosin heavy-chain modulate myosin functional properties (Murphy and Spudich, 2000; Swank et al., 2000). However, the importance of these domains toward setting muscle mechanical properties has only recently been directly tested in organized muscle systems (Babu et al., 2001; Swank et al., 2002).

Using the genetic advantages of the *Drosophila* system, we can directly measure the influence of various muscle protein isoforms and mutations on indirect flight and jump muscle performance (Maughan and Vigoreaux, 1999; Peckham et al., 1990; Swank et al., 2000). The availability of various muscle-specific protein nulls and techniques such as *P*-element-mediated transformation, allows for the transgenic replacement of specific proteins in selected muscles (Cripps and Bernstein, 2000). This was demonstrated for myosin heavy chain (MHC) by transgenic expression of an embryonic (EMB) MHC in *Drosophila* indirect flight muscle (IFM), which resulted in loss of flight ability (Wells et al., 1996). The EMB and IFI isoforms differ at all four S1

variable regions (Fig. 1) and are functionally distinct in vitro (Swank et al., 2001). Swank et al. (2002) subsequently showed that substitution of the EMB isoform for the native IFI isoform transformed the IFM from a high power-generating muscle that works optimally at high oscillation frequencies to one that produces less power and functions best at low oscillation frequencies. Hence fibers expressing EMB are too slow to power flight.

The *Drosophila* system is especially valuable for structure/function studies of MHC due to *Drosophila's* mechanism of MHC isoform expression. In *Drosophila*, a diverse array of MHC isoforms are generated through alternative splicing of mRNA transcripts from the single copy *Mhc* gene (Bernstein et al., 1983; George et al., 1989; Rozek and Davidson, 1983). Fifteen isoforms have been identified to date, expressed in a wide variety of fiber types including the supercontractile embryonic body wall muscles and the extremely fast indirect flight muscle (Hastings and Emerson, 1982; Zhang and Bernstein, 2001). There are five sets of alternatively spliced exons in *Mhc*, four in the head region alone. Mapping the location of the alternative exons on the atomic resolution three-dimensional MHC structure directs us to regions of the molecule that must be used to set specific myosin properties and hence likely to influence fiber mechanical performance (Bernstein and Milligan, 1997). In contrast, for vertebrate myosin isoforms it is difficult to identify structural regions that determine functional properties because of the large number of MHC genes and amino acid differences between MHC isoforms.

Thus far, two regions, exons 3 and 11, have been shown to influence functional differences between *Drosophila* myosin isoforms (Swank et al., 2002, 2003). The region encoded by
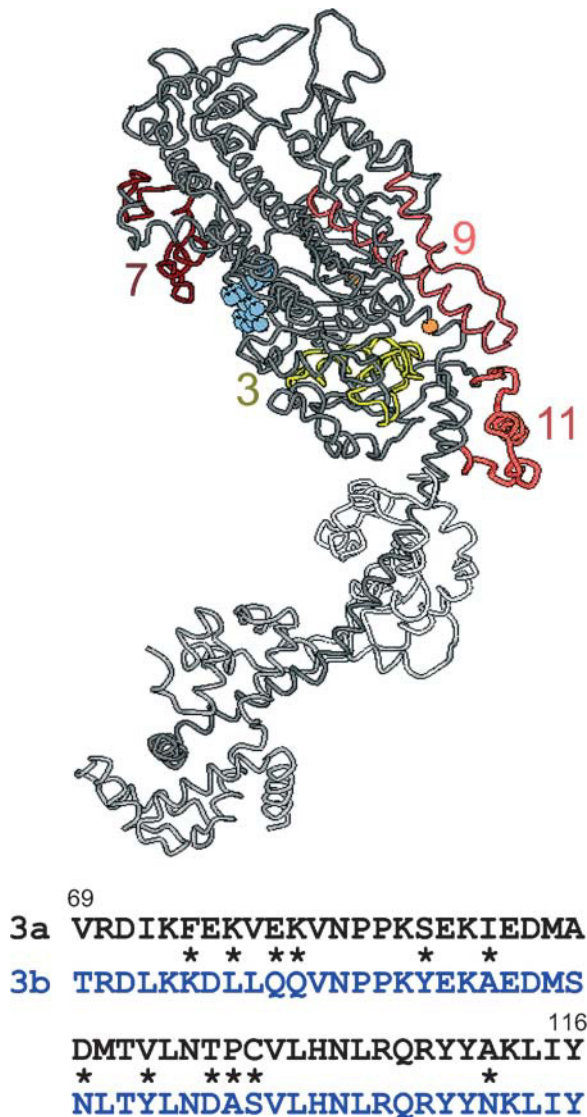
FIGURE 1 Location and alternative sequence choices for the exon 3 region. The exon 3 region (*yellow*) and the three other variable regions (7, 9, and 11) encoded by *Drosophila* alternative exons (shades of *red*) are mapped onto the chicken myosin S1 structure (*gray*). The exon 3 region is located near the reactive sulfhydrils (*orange*) and near the point about which the light-chain region (light chains in *light gray*) pivots in response to ADP release (Bernstein and Milligan, 1997). The blue spheres depict ADP in the active site. The two alternative amino acid sequences of the exon 3 region are shown below the molecular structure. *Signifies nonconserved substitutions.

exon 3 is located near the N-terminus between the active site and the pivot point of the lever arm; this corresponds to residues 69–116 of chicken skeletal MHC (Fig. 1). There are two alternative choices for exon 3 that differ in 17 of 48 amino acids, 12 of which are nonconserved substitutions (Bernstein and Milligan, 1997). One version, 3b, is expressed primarily in adult muscles, including the very fast indirect flight muscle and a few embryonic body wall muscles. The other, 3a, is expressed only in embryonic muscles, including most intermediate and internal body wall muscles, visceral muscle, and embryonic cardioblasts (Zhang and Bernstein, 2001).

We previously characterized the effect of this region on myosin ATPase rates and actin sliding velocity by exchanging the exon 3 region between the IFI and EMB myosin isoforms (Swank et al., 2003). This created two myosin chimeras referred to as IFI-3a (flight muscle isoform with the EMB version of exon 3, 3a) and EMB-3b (the EMB isoform with the IFI version of exon 3, 3b). We found that the two structural versions of the exon 3 domain independently influence ATPase rates and actin sliding velocity, suggesting that each alternative exon independently influences different steps or rate constants of the cross-bridge cycle. Expressing the chimeras in the flight muscle caused subtle differences in flight ability. For example, the IFI-3a lines fly, but are not able to fly up as well as IFI flies (Swank et al., 2003). The reduced flight ability suggests a decrease in power generation from IFI-3a flight muscle fibers.

To determine the influence of the exon 3 encoded domain on muscle power generation and mechanical properties, we assessed the mechanical performance of IFM fibers expressing genetically altered myosin heavy chain isoforms. The ability to make this assessment is unique to the *Drosophila* system. Our results revealed that this region can account for a significant portion of the striking mechanical differences observed between IFI and EMB expressing IFM fibers. Comparing our current mechanics results and previously reported myosin molecular properties (Swank et al., 2003) allowed us to draw functional correlations. Finally, we performed flight and wing beat frequency testing on IFI-3a flies at the same temperature as the mechanical measurements to reveal a fully integrative functional picture of this region of myosin.

METHODS

Creation of the EMB transgenic line is described in Wells et al. (1996) and construction of lines expressing the exon 3 chimeras is described in Swank et al. (2003). Transgenes were inserted into the *Drosophila* germline by *P*-element-mediated transformation (Cripps and Bernstein, 2000). RT-PCR and SDS-PAGE confirmed that all transgenes properly expressed the expected protein (Swank et al., 2003). Fibers from two independent *Drosophila* lines generated from the EMB (EMB and EMB, 34) and EMB-3b (EMB-3b and EMB-3b, 157) transgenes were mechanically evaluated to rule out the possibility of a transgene inserting into a gene that affects flight muscle function. Mechanical measurements of fibers from an IFI line produced results identical to the independently generated IFI line reported on in Swank et al. (2002). Because two independently generated IFI-3a lines (IFI-3a and IFI-3a, 7) had identical flight ability and wing beat frequencies (Table 4), we carried out a mechanical evaluation on only one IFI-3a line.

Electron microscopy

Using transmission electron microscopy, we evaluated whether the ultrastructure of the transgenic IFMs was suitable for meaningful mechanics experiments. Details of fixation, osmium staining, embedding, and thin sectioning are described in O'Donnell and Bernstein (1988).

Mechanics protocol

A bundle of six IFM fibers was dissected from a half-thorax. Fibers were separated and a single fiber split lengthwise producing a preparation ~100

μm in diameter and $\sim$0.6 mm in length. Fibers were chemically demembranated (skinned) in a relaxing solution (5 mM MgATP, 15 mM creatine phosphate, 240 U/ml creatine phosphokinase, 1 mM free Mg^{2+}, 5 mM EGTA, 20 mM BES (pH 7.0), 200 mM ionic strength, adjusted with Na methane sulfonate, 1 mM DTT, and 50% glycerol) containing 0.5% Triton X-100, for 1 h at 4°C. Aluminum T-clips were used to mount the fibers on a mechanical rig (Dickinson et al., 1997), and the temperature was set at 15°C. The fiber was stretched until just taut and then lengthened by 1% muscle length increments until it reached 5% of just taught length. Sinusoidal analysis (next section) was performed while the fiber was in relaxing solution. The fiber was activated to pCa 5.0 by three partial solution exchanges of the initial relaxing solution with activating solution (same as relaxing but calcium content adjusted to pCa 4.0). Sinusoidal analysis was performed in activating solution. The fiber was stretched by 2% muscle length increments until work output, as determined by sinusoidal analysis was maximal (typically requiring a total stretch of 6%). Relaxing solution was then exchanged into the chamber, tension measured, and step and sinusoidal analysis repeated. Rigor tension was measured in a bathing solution of activating solution minus ATP, creatine phosphokinase, and creatine phosphate.

Sinusoidal analysis

Sinusoidal analysis was performed as in Dickinson et al. (1997). Briefly, sinusoidal length changes of 0.25% muscle length (peak to peak) were applied over 47 frequencies from 1 to 1000 Hz to the fiber. For each frequency, the elastic and viscous moduli were calculated from the length and force transients by computing the amplitude ratio and the phase difference for force and length. The ratio was divided by fiber cross-sectional area. *Work* $(Jm^{-3}) = \pi E_v (\Delta L/L)^2$ and *Power* $(Wm^{-3}) = \pi f E_v (\Delta L/L)^2$, where f is the frequency of the length perturbations (s^{-1}), E_v is the viscous modulus at f, and $\Delta L/L$ is the amplitude of the sinusoidal length change divided by the length of the fiber between the two T-clips.

Step analysis

To determine the rate of tension redevelopment (r_3), activated fibers were subjected to a series of four identical 0.5% muscle-lengthening steps. The force response was averaged over the four steps. The force response was fit to the sum of three exponential curves: $a_1[1 - \exp(-k_1 t)] + a_2 \exp(-k_2 t) + a_3 \exp(-k_3 t) + $ offset. Constants a_1, a_2, a_3 are amplitudes; k_1, k_2, and k_3 are rate constants; k_1 is r_3. The offset adjusts for nonzero starting values.

Flight assays

Flight ability and wing beat frequency were measured at 15°C, the same temperature at which muscle mechanical measurements were performed, to allow direct comparison of muscle kinetics and flight parameters. Wing beat frequency was also measured at 22°C. Wing beat frequency of a tethered fly was determined using an optical tachometer (Hyatt and Maughan, 1994). Flight ability was assayed by observing whether a fly is capable of flying up (U), horizontal (H), down (D), or not at all (N) when released in a plexiglass flight chamber (Drummond et al., 1990). Flight index equals $6U/T + 4H/T + 2D/T + 0N/T$, where T is the total number of flies tested (Tohtong et al., 1995). Flight ability at 22°C is from Swank et al. (2003).

RESULTS

Ultrastructural integrity of myofibrils expressing chimeric myosins

Previously, we found that EMB-3b fibers at 2 days of age exhibit significant myofibril disarray (Fig. 2 *A*), although
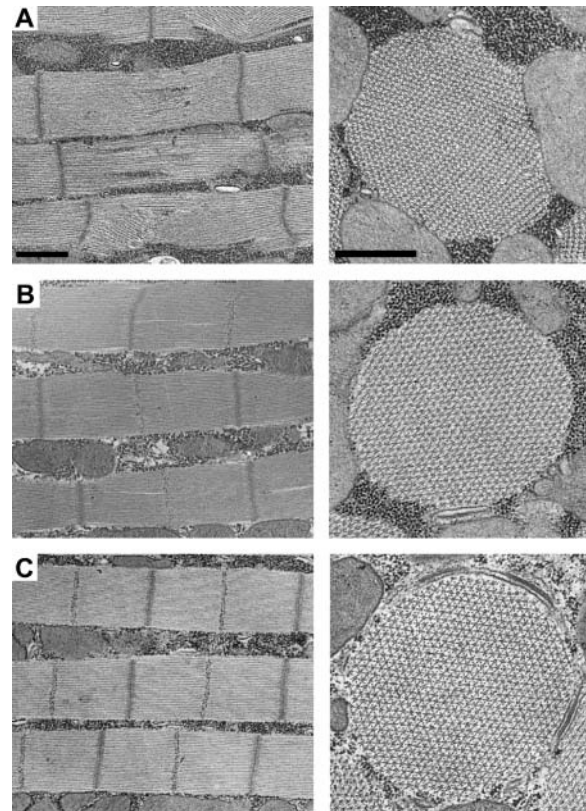

FIGURE 2 IFM myofibril ultrastructure stability. All panels display longitudinal (*left*) and transverse (*right*) views of DLMs (the medial set of the two opposing sets of IFMs). Scale bar lengths are both 0.5 μm. (*A*) EMB-3b IFMs of 2-day-old adults exhibit ultrastructure abnormalities (Swank et al., 2003). (*B*) EMB-3b IFMs of <2-h-old adults. At this age the myofibrils show only very slight indications of ultrastructure abnormalities. (*C*) IFMs from <2-h-old adults expressing IFI myosin.

much less severe than EMB fibers at that age (Swank et al., 2003). In an effort to obtain an EMB-3b preparation that was structurally amenable to mechanical studies, we compared fibers that were <2 h old to IFI fibers of the same age (IFI-2h) (Fig. 2, *B* and *C*). We found that the 2-h-old EMB-3b fibers are dramatically improved compared to EMB or EMB-3b fibers at 2 days. Both cross sections and longitudinal sections are nearly indistinguishable from wild type, with an occasional misaligned thick filament, similar to that seen in EMB fibers. Thus, like EMB fibers, EMB-3b appears to assemble essentially normally, but undergo progressive degradation. Both have yielded reproducible mechanical data at <2 h (see following sections and Swank et al., 2002), before the onset of this degradative process. Swank et al. (2003) showed that the ultrastructure of 2-day-old IFI-3a fibers is indistinguishable from IFI fibers.

It is possible that, similar to the damage occurring during aging, damage to EMB and EMB-3b fibers is occurring during the course of our experiments due to the kinetic mismatch between very fast IFM fibers and the slow myosin isoforms. To assess this possibility, we compared maximum values of the viscous modulus (i.e., maximum work output)

and power generation at the start of the experiment with values obtained under the same conditions near the end of the experiment. The measurements were made ~45 min apart, with at least 10 runs between the identical experimental conditions. All fibers showed an ~5% decrease in work generation and ~8% decrease in power generation (Table 1), with only very slight (<5%) reductions in fE_v and f_{max}, suggesting minimal rundown or deterioration of the fiber during the experiment. The EMB and EMB-3b lines did not show any significant difference compared to the IFI control. These results suggest that if any ultrastructural damage is occurring during the mechanical measurements, it has no appreciable effect on our mechanical measurements.

The diameter of 2-h-old *Drosophila* myofibrils is less than that of 2-day-old myofibrils as IFM development continues for at least several hours after eclosion, with additional thick and thin filament accumulation (Reedy and Beall, 1993). The reduced number of filaments per myofibril resulted in lower power, tension, and work values from young fibers, as evident from our experiments on <2-h-old IFI control fibers (denoted IFI-2h) compared to 2-day-old IFI fibers (Tables 2 and 3). Thus any mechanical values that are normalized to fiber cross-sectional areas should only be compared to fibers of a similar age. In contrast, the kinetics of IFI and IFI-2h were similar; thus kinetic properties, such as the frequency of maximum power generation (f_{max}) (Table 2), can be compared across all lines.

Mechanics analysis of transgenic IFM fibers

Complex stiffness and phase

Sinusoidal analysis revealed differences in the complex stiffness of the chimeric fibers compared to their parent fibers. The IFI-3a phase plot was shifted to the left compared to IFI suggesting a slowing in overall fiber kinetics. IFI-3a complex stiffness amplitude was not significantly different from IFI over all frequencies tested (Fig. 3 *A* and Table 2). Comparing complex stiffness of EMB-3b and EMB (Fig. 3 *B* and Table 2) we see a more dramatic difference than IFI compared to IFI-3a. EMB-3b complex stiffness was higher at almost all frequencies tested than EMB. The EMB-3b phase plot was shifted to the right indicating an increase in speed of fiber kinetics compared to EMB. However, the increase in

kinetics was only ~25% of the difference between the EMB and IFI-2h values.

Elastic and viscous moduli

Separating the complex stiffness into its elastic and viscous components (Fig. 4) revealed which observed differences in complex stiffness are primarily due to active force generating or absorbing processes (*viscous modulus*), and which are primarily due to differences in passive muscle elements (*elastic modulus*). Differences between IFI and IFI-3a occurred over the frequency range where work was produced by the fiber (negative viscous modulus). The minimum amplitudes of IFI-3a's modulus were shifted leftward to lower frequencies compared to IFI. This was especially apparent in the viscous modulus plot (Fig. 4 *B*). This suggests that IFI-3a myosin operates better at lower muscle oscillation frequencies than IFI. However, the minimum amplitude of the viscous modulus of the two fibers was not significantly different (Table 2). Because muscle length change for both fibers was identical at all frequencies, maximum work per cycle is proportional to the viscous modulus (E_v). Thus the IFI and IFI-3a fibers generated an equal amount of maximum work per cycle, but at different frequencies (Table 2, fE_v). The elastic modulus of IFI-3a fibers was 78% of the IFI elastic modulus over the frequency range of 100–200 Hz (Fig. 4 *A* and Table 2, E_e). This decrease in stiffness may influence wing beat frequency (see Discussion below).

For EMB-3b compared to EMB, we saw a rightward shift in both the elastic and viscous moduli (Fig. 4), suggesting that EMB-3b fibers operate best at faster oscillation speeds than EMB fibers. The EMB-3b elastic modulus was stiffer (greater) than that of IFI-2h and EMB-3b at most frequencies (Fig. 4 *A*). The viscous modulus dips lower than EMB or IFI-2h suggesting EMB-3b produced more work, which was confirmed by comparing the minimum viscous modulus amplitude ($-Ev$) for EMB-3b, EMB, and IFI-2h fibers (Table 2). The greater viscous modulus of EMB-3b at higher frequencies suggests it is capable of absorbing more work than EMB or IFI-2h (Fig. 4 *B*). The higher elastic modulus at almost all frequencies shows the IFI-3a fiber is also capable of recovering more work than EMB. The increased elastic modulus, viscous modulus, and complex stiffness suggest

TABLE 1 Percent decrease in mechanical properties from start to end of experiment

	Number	$-E_v$ (kN/mm^2)	fE_v (Hz)	P_{max} (W/m^3)	f_{max} (Hz)
IFI	9	-5.6 ± 3.4	-4.8 ± 4.6	-9.7 ± 2.9	-0.3 ± 1.5
IFI-3a	8	-3.2 ± 1.9	-3.7 ± 7.3	-8.9 ± 4.8	-6.9 ± 4.4
EMB, 34	9	-6.9 ± 5.8	-5.6 ± 4.1	-8.3 ± 6.7	-3.7 ± 4.2
EMB-3b	8	-6.4 ± 3.4	-1.1 ± 3.8	-7.0 ± 5.2	-1.8 ± 1.8
EMB-3b, 157	8	-7.5 ± 4.2	-2.6 ± 4.7	-11.7 ± 3.1	-2.6 ± 3.7
IFI-2h	5	-4.2 ± 3.4	-3.4 ± 2.1	-7.9 ± 4.5	-1.7 ± 2.4

EMB, 34 is a second EMB line created by an independent transformation event, and EMB-3b, 157 is a second EMB-3b line created by an independent transformation event. All values are means ± SE.

TABLE 2   Summary of dynamic properties

	N	C. stiff (kN m^{-2})	$-E_v$ (kN m^{-2})	fE_v (Hz)	E_e (kN m^{-2})	P_{max} (W/m^{-3})	f_{max} (Hz)	r_3 (s^{-1})
IFI	10	367 ± 28	142 ± 12	125 ± 4	343 ± 23	81 ± 8	145 ± 4	1140 ± 66
IFI-3a	10	283 ± 34*	134 ± 24	78 ± 5[†]	267 ± 28[‡]	56 ± 9[†]	121 ± 4[†]	797 ± 55[†]
EMB	7	74 ± 13	51 ± 10	18 ± 0.9	58 ± 10	4.4 ± 0.9	19 ± 0.8	111 ± 7
EMB, 34	6	70 ± 12	42 ± 8	17 ± 1.1	61 ± 9	3.6 ± 0.8	18 ± 1.1	108 ± 4
EMB-3b	7	164 ± 18[§]	80 ± 12[§]	31 ± 1.7[§]	146 ± 14[§]	12 ± 1.9[§]	34 ± 0.9[§]	295 ± 27[§]
EMB-3b, 157	6	158 ± 11[§]	83 ± 6[§]	27 ± 1.7[§]	134 ± 11[§]	11 ± 0.8[§]	30 ± 0.7[§]	312 ± 8[§]
IFI-2h	5	135 ± 9[§]	34 ± 2	132 ± 4[§]	132 ± 9[§]	22 ± 2[§]	152 ± 6[§]	1169 ± 58[§]

Complex stiffness (*C. stiff*) and elastic modulus (E_e) values for IFI and IFI-3a were measured at the frequency (f_{max}) at which IFI generated maximum power (P_{max}). E_e and *C. stiff* values for EMB, EMB-IC, and IFI-2h were measured at the specific f_{max} of each fiber type. fE_v is the average frequency at which the viscous modulus amplitude was lowest. $-E_v$ is the average minimum amplitude for the viscous modulus, and r_3 is the rate constant for phase 3 of force recovery after a quick lengthening step (see Methods). EMB, 34 is a second EMB line created by an independent transformation event, and EMB-3b, 157 is a second EMB-3b line created by an independent transformation event. All values are means ± SE.
*t-test, $p = 0.073$ for IFI compared to IFI-3a.
[†]Statistically different from IFI (t-test, $p < 0.05$).
[‡]t-test, $p = 0.047$ for IFI compared to IFI-3a.
[§]Statistically different from EMB and EMB, 34 (t-test, $p < 0.05$).

that substituting exon 3a into EMB increased myosin cross-bridge stiffness.

Power generation

The impact of the exon 3 exchange on power generation was quite striking (Fig. 5). At 15°C, IFI-3a maximum power (P_{max}) occurred at 121 Hz compared to 145 Hz for IFI (Table 2; Fig. 5 *a*). P_{max} for IFI-3a fibers was ~70% of IFI (Table 2). Dramatic differences in power-producing ability for IFI-3a occurred over the frequency range of 175–220 Hz where IFI fibers generated power, but IFI-3a fibers were no longer capable of generating power. At lower frequencies, 20–110 Hz, power production by IFI-3a was equal to or slightly higher than IFI. At the average wing beat frequency of IFI flies, power generation of IFI-3a fibers was only 60% of IFI (Fig. 5 A, *right vertical dashed line*).

The effect of the IFI exon 3 region on EMB power generating ability was even more impressive. EMB-3b frequency of maximum power generation (f_{max}) was 1.8-fold greater than EMB, and P_{max} increased almost threefold (Fig. 5 *B*; Table 2). Above 20 Hz EMB-3b power production was much greater than EMB. EMB cannot generate power

TABLE 3   Isometric properties

	N	T_{max} (mN/mm^2)	Passive tension (mN/mm^2)	Rigor tension (mN/mm^2)
IFI	8	1.32 ± 0.12	2.0 ± 0.2	2.9 ± 0.2
IFI-3a	8	1.72 ± 0.22	2.6 ± 0.4	3.9 ± 0.3*
EMB	7	0.97 ± 0.20	0.7 ± 0.2	1.6 ± 0.3
EMB-3b	7	0.80 ± 0.07	0.9 ± 0.1	3.4 ± 0.7[†]
IFI-2h	5	0.36 ± 0.05[‡]	1.1 ± 0.2	1.3 ± 0.2

T_{max} = net active tension (gross active tension minus passive tension). Rigor tension = net rigor tension (gross rigor tension minus passive tension). All values are means ± SE.
*Statistically different from IFI, (t-test, $p = 0.043$).
[†]Statistically different from EMB and IFI-2h, (t-test, $p < 0.05$).
[‡]Statistically different from EMB and EMB-3b (t-test, $p < 0.05$).

above 25 Hz, whereas EMB-3b generated useful power up to 45 Hz. Above 50 Hz, EMB-3b muscle was not capable of producing useful power. Its useful range was approximately fourfold lower than the wing beat frequency range capable of supporting *Drosophila* flight (~120–160 Hz at 15°C).

Rate of force redevelopment, r_3

To confirm the differences in fiber kinetics seen with sinusoidal analysis, we employed a more traditional measure, step analysis (Ford et al., 1977; Steiger, 1977). We confirmed our previous finding that the rate of tension regeneration of EMB is one-tenth that of IFI (Fig. 6; Table 2). Exchanging EMB exon 3 into IFI caused r_3 to slow to 76% of IFI. Conversely, EMB-3b r_3 more than doubled compared to EMB r_3. This closely resembled the differences in f_{max} observed with sinusoidal analysis (Table 2).

Isometric tension

We previously reported that EMB can generate more isometric tension than IFI (Swank et al., 2002), which we confirmed in this study by observing a 2.7-fold higher EMB fiber tension than IFI-2h fiber tension (Table 3, T_{max}). However, the exon 3 region did not appear to significantly influence isometric tension. Although IFI-3a isometric tension tended to be greater than that of IFI and EMB-3b tension less than that of EMB, neither difference was statistically significant. We did observe significant increases in rigor tension for both chimeras compared to their respective parent isoforms (Table 3).

Flight ability

Previously, we observed that IFI-3a *Drosophila* are not able to fly upwards as well as IFI *Drosophila* (Table 4, column 1). To investigate the basis for this impairment, we measured wing
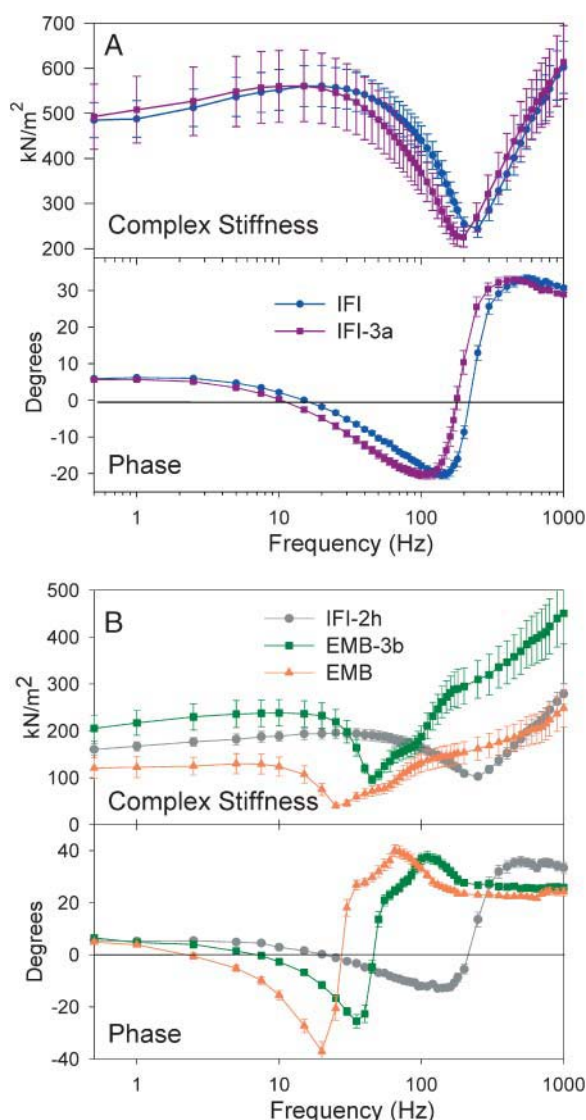
FIGURE 3 Complex stiffness and phase shift of maximally Ca^{2+}-activated IFM fibers at 15°C. (*A*) Complex stiffness and phase as a function of frequency for IFI and IFI-3a IFM fibers from 2-day-old flies. (*B*) Complex stiffness and phase as a function of frequency for IFI-2h, EMB-3b, and EMB fibers from <2-h-old adults. Note the different *y* axis scales for complex stiffness in panels *A* and *B* as fibers from the younger flies have less myofibril area per cross section (see text).

beat frequency (*WBF*) at 22°C and found that IFI-3a wing beat frequency was 89% of IFI *WBF* (Table 4, column 2). This would decrease IFI-3a aerodynamic power, as power is proportional to the third power of *WBF* (Laurie-Ahlberg et al., 1985).

To enable direct comparison between fiber mechanical studies and flight performance, we measured flight ability at the same temperature, 15°C, that we performed fiber mechanics. At 15°C, flight ability of IFI-3a was severely impaired compared to IFI. IFI-3a flight index dropped to 1.5 whereas IFI remained at 4 (Table 4, column 3). Wing beat frequency of IFI-3a was 87% of IFI *WBF* (Table 4, column 4). Both *WBF* values at 15°C were 78% of their respective values

at 22°C (compare columns 2 and 4, Table 4). The flight ability and *WBF* phenotypes were corroborated in a second, independently generated, transgenic IFI-3a line, 7 (Table 4).

Neither EMB nor EMB-3b *Drosophila* can fly at any temperature. This is not surprising because fibers from these lines are not able to generate power when oscillated at frequencies corresponding to frequencies that support flight.

DISCUSSION

Differences between IFI and EMB control fibers

Previously, we directly proved that myosin isoforms are the primary determinant of *Drosophila* muscle kinetics (Swank et al., 2002). Substitution of the EMB isoform for the native isoform transformed the IFM from a high-power-generating muscle that performs optimally at high oscillation frequencies to one that produces less power and functions best at low frequencies. Specifically, EMB fibers generate only 25% of the maximum power (P_{max}) of IFI fibers at 15% of IFI f_{max}. Maximum work is almost twofold higher in EMB, and frequency of maximum work production (Wf_{max}) occurs at 30% of IFI Wf_{max} (Littlefield et al., 2003). The large kinetic differences measured by sinusoidal analysis were corroborated by step analysis, where the rate of tension redevelopment, r_3, for EMB was only 10% of IFI (Littlefield et al., 2003; see also Fig. 6). Isometric tension generation was almost threefold higher in EMB than IFI fibers (Swank et al, 2002). Our current measurements (using a separate IFI transformant line as a source for IFI fibers and different EMB fibers) verified these results. Further, this analysis found differences in complex stiffness parameters between IFI and EMB, with contributions from both viscous and elastic components.

A striking difference between EMB and IFI was a dramatic variation in the shape of the elastic and viscous moduli at higher frequencies, where the fibers are net absorbers of work (positive viscous modulus) (Fig. 4, *A* and *B*). The low-frequency ranges of the EMB and EMB-3b (<60 Hz and <100 Hz, respectively) viscous moduli are shaped very similarly to IFI-2h, only compressed such that they span lower frequencies. According to the interpretation of Kawai and Brandt (1980) and others (Blanchard et al., 1997; Mulieri et al., 2002), the high-frequency alteration is evidence for an extra cross-bridge ''process''. This extra process most likely represents either a very rapid myosin isomerization that changes the stiffness of the cross-bridge, or a very fast transition between differing strength actin binding states. The transition/isomerization must occur faster or be shorter lived than the work producing transition because it is observed at much higher oscillation frequencies. This extra process is absent in the faster fibers, either because the transition rate is too fast to be observed (i.e., faster than 1000 Hz) or the transition/cross-bridge state does not exist in the cross-bridge cycle of the faster isoforms. Because the moduli of EMB-3b and IFI-3a chimeras had similar shapes as their respective
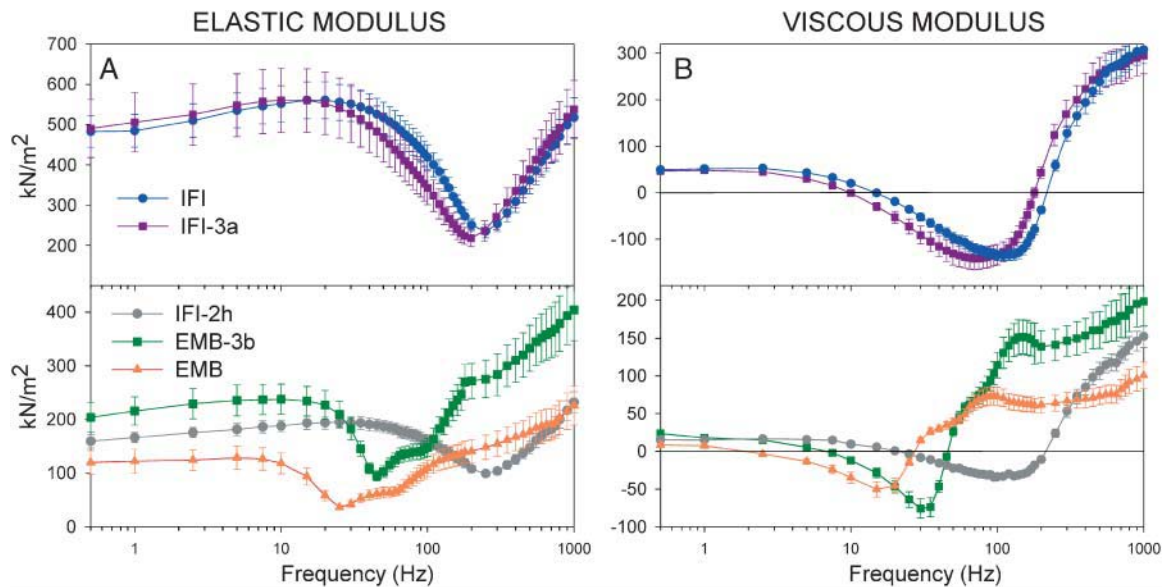
FIGURE 4 Elastic and viscous moduli of maximally Ca^{2+}-activated IFM fibers. (*A*) Elastic modulus (instantaneous stiffness) as a function of frequency for all five fiber types. (*B*) Viscous modulus as a function of frequency for all five fiber types.

parent isoforms, the exon 3 region probably does not determine if the fiber has this extra process.

Molecular basis for influence of exon 3 on muscle mechanical properties

Our results show definitively that the amino acid differences between the exon 3 encoded regions play an important role in setting fundamental kinetic characteristics of the IFI and EMB transgenic fiber types such as differences in f_{max}, r_3, and the phase versus frequency curve. Differences in magnitude of the elastic and viscous modulus may reflect alterations in stiffness of the myosin cross-bridge itself due to structural alterations from differential expression of exon 3. Alternatively, changes in myosin kinetics that influence how long the myosin spends in strongly bound states versus weakly bound states, i.e., duty ratio (see below), could influence the magnitudes of the moduli.

Our previous results from studying the biochemistry and biophysics of isolated IFI-3a and EMB-3b myosin chimeras allows for correlations between molecular properties and fiber kinetics. Of significant interest, one exon 3 exchange altered in vitro actin sliding velocity whereas the other exon 3 exchange only altered ATPase rates, suggesting independent effects on different cross-bridge rate constants (Swank et al., 2003). Specifically, EMB-3b had a 5.4-fold increase in actin velocity compared to EMB, but no increase in actin-activated ATPase V_{max}. Conversely, IFI-3a ATPase V_{max} slowed to EMB levels (100% of the difference between EMB and IFI) without a change in actin sliding velocity.

The IFI-3a fiber's kinetics only decreased approximately one-quarter of the way to the EMB fiber kinetics. Given that, at the molecular level, the ATPase rate dropped to EMB

levels, this suggests that the steps of the cycle that set ATPase rate in solution (thought to be limited by a weak-to-strong actin-binding isomerization associated with Pi release; Geeves, 1991) only play a minor role in determining fiber kinetics. The small impact of variation in myosin ATPase rates to overall insect fiber kinetics is supported by Molloy et al. (1987) who found that fiber ATPase rate does not vary significantly among insect flight muscles from different species, even though large differences in fiber kinetics are observed. However, although our data suggest that the rate constants that set in vitro actin velocity (typically thought to be limited by steps associated with ADP release rate; Spudich, 1994) are more important to fiber kinetics, they are not sufficient to set oscillatory fiber kinetics because the EMB-3b increase in actin sliding velocity was greater than the observed increase in fiber kinetics.

We previously found that duty ratio (the percent of total cross-bridge cycle time myosin spends bound to actin, estimated from actin-activated ATPase V_{max} and actin sliding velocity) differed greatly for EMB and IFI (Littlefield et al., 2003). For our exon 3 chimeras, both IFI-3a and EMB-3b duty ratios would be predicted to be less than the respective parent isoforms. Isometric tension should thus decrease because it is proportional to duty ratio (Littlefield et al., 2003). However, no significant difference in isometric tension was observed. Previously, we reported that exchanging the alternative versions of exon 11 (the converter domain) between IFI and EMB resulted in differences in isometric tension that correlated with duty ratio predictions (Littlefield et al., 2003). The exon 11 exchange produced much greater changes in in vitro motility, ATPase rates, and fiber f_{max} than observed for the exon 3 exchanges. Thus it may be that the kinetic changes in myosin molecular properties from the exon 3 exchange are not
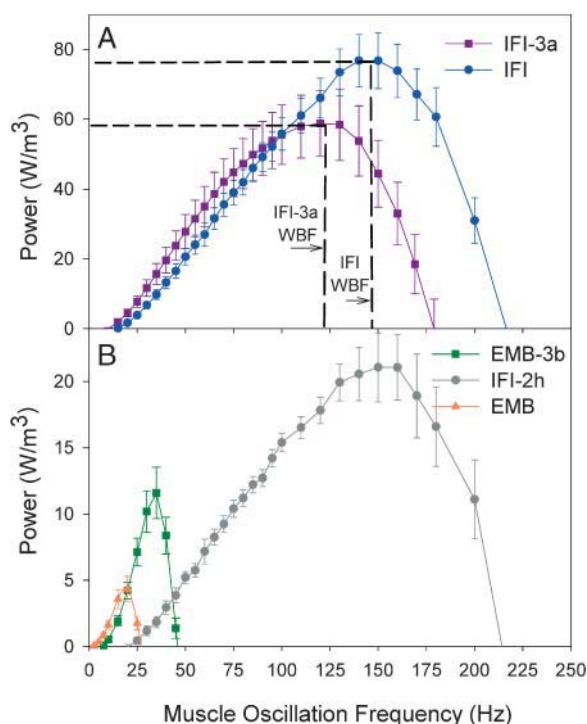
FIGURE 5 Power generation by maximally activated IFM fibers at 15°C. (*A*) Power generated by IFI and IFI-3a muscle fibers when oscillated at 0.25% peak-to-peak strain over a frequency range of 0.5–250 Hz. Wing beat frequency (*WBF*) for each transgenic line (Table 4) is indicated (*vertical dashed lines*) at the corresponding muscle oscillation frequency. By beating their wings at a slower frequency, IFI-3a flies generate more power from their IFMs than if *WBF* remained at the higher IFI *WBF*. (*B*) Power generated by EMB-3b, IFI-2h, and EMB fibers as a function of frequency. EMB and EMB-3b fibers cannot generate power over the normal range of wing beat frequencies that support flight. The IFI-2h fibers (from flies <2 h old) have the same f_{max} as IFI, but generate only 27% as much power as adults. This is due to the young fibers having less thick and thin filaments per fiber cross section (see text). If EMB-3b power generation was normalized to IFI levels (based on IFI-2h P_{max} compared to IFI P_{max}), EMB-3b P_{max} would be ~43 W/m³, which would be less than IFI-3a P_{max}.

of sufficient magnitude to be observed by our method of isometric tension measurement. Alternatively, the exon 3 exchanges may increase unitary force production (step-size × cross-bridge stiffness) of the cross-bridge. The possibility that cross-bridge stiffness increases is supported by the increased rigor tension for IFI-3a and EMB-3b that was observed compared to IFI and EMB, respectively, and by the higher complex stiffness of EMB-3b compared to EMB (Table 2). An increase in cross-bridge stiffness or step-size would counter the predicted decrease in duty cycle (isometric force duty cycle × step-size × cross-bridge stiffness × number of cross-bridges recruited), which could underlie the lack of significant differences in isometric force. A resolution of these alternate possibilities awaits further mechanical and single molecule assays.

The region encoded by exon 3, to our knowledge, has not been the subject of previous mutagenesis studies to resolve myosin structure/function relations. However, evidence for
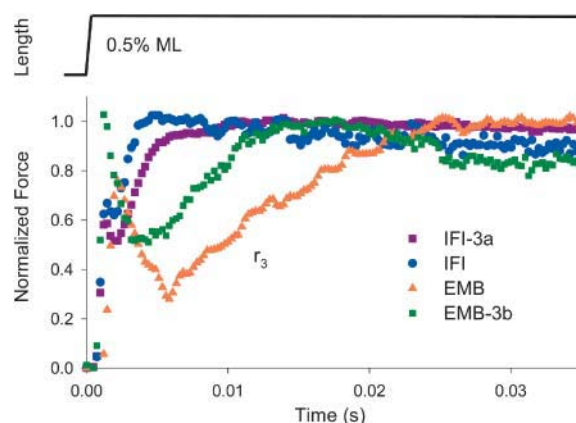

FIGURE 6 Rates of tension redevelopment (r_3). IFM fibers at pCa 5.0 were subjected to a rapid lengthening step, 0.5% muscle length. Representative traces of IFI-3a, IFI, EMB, and EMB-3b are shown with tension levels normalized to maximum tension immediately after phase 3.

environmental change around or movement of this region was suggested by Kovacs et al. (2002) who observed an increase in fluorescence and a 2-nm red shift in the emission from Trp-113 (located in the exon 3 encoded region) upon ADP and ATP binding in *Dictyostelium* myosin. This suggests movement of the region is coordinated with activity at the nucleotide binding site and raises the possibility that this portion of the exon 3 encoded region could be involved in setting ATPase rates. Further, Burghardt et al. (2001) propose that amino acids 84 and 85 (located on the opposite side of the exon 3 domain from Trp-113) interact with the converter region and/or lever arm during or after the power stroke, based on optical spectroscopic signals from extrinsic probes bound to rabbit S1. Before the MgADP state, exon 3 only interacts with other portions of the catalytic domain, but in the MgADP and rigor states, it is in close proximity to the converter domain and the portion of the lever arm adjacent to the catalytic domain (Burghardt et al., 2001). Perhaps this area of exon 3 is involved in setting actin sliding velocity.

The fiber kinetic differences between IFI and EMB attributable to the exon 3 region are only a small percentage of the overall kinetic differences between IFI and EMB, suggesting that other alternative exons must play a role in setting fiber mechanical properties. In particular, we previously found that the converter region, encoded by exon 11, has a major influence on fiber kinetics (Swank et al., 2002; Littlefield et al., 2003). The question arises whether the combined influence of exons 3 and 11 is enough to convert the kinetics of one native fiber type to the other. Independently, the IFI alternative exon versions of 11 and 3 each cause a doubling of EMB f_{max}. If the influences are additive, one would expect at least a fourfold increase in f_{max} (to ~80 Hz) about half-way to IFI f_{max} (145 Hz). Conversely, the EMB version of 11 decreased IFI f_{max} half-way to EMB (50% of IFI), whereas the EMB version of exon 3 only decreased f_{max} to 80% of IFI. Thus, either the combined effect of exchanging

TABLE 4 Flight characteristics

	Flight index, 22°C	Wing beat frequency, 22°C	Flight index, 15°C	Wing beat frequency, 15°C
IFI	4.0 ± 0.2 (100)*	181 ± 2 (12)	3.9 ± 0.3 (39)	148 ± 2.1 (14)
IFI-3a	3.0 ± 0.2 (100)*[†]	162 ± 3 (13)[†]	1.5 ± 0.2 (43)[†]	129 ± 1.9 (21)[†]
IFI-3a, 7	2.9 ± 0.2 (100)[†]	161 ± 4 (6)[†]	1.2 ± 0.3 (28)[†]	128 ± 3.7 (7)[†]

All values are means ± SE. Numbers in parentheses = number of flies tested. IFI-3a, 7 is a second, independently generated, transgenic IFI-3a line.
*Data from Swank et al. (2003).
[†]Statistically different from IFI (*t*-test, $p < 0.05$).

exons 11 and 3 is greater than their sum, or one or more of the remaining two alternative exons also contribute to fiber kinetic differences.

Influence of exon 3a on *Drosophila* flight ability

Although the exon 3 encoded region does not have a dominant effect on fiber kinetics, its influence is physiologically significant as seen by its important role in dictating flight ability (Table 4). To understand the relationship between muscle power, wing beat frequency, and flight ability, we plotted the *WBF* of IFI and IFI-3a at 15°C on the IFI and IFI-3a muscle power generation curves (also performed at 15°C) (Fig. 5 *A*). *WBF* at 15°C for IFI is at the peak of the power curve, almost identical to IFI f_{max}. Although it has been shown that muscle f_{max} does not set *Drosophila WBF* (Swank et al., 2002) (rather the muscle must oscillate at the wing beat frequency, which is set by the resonant properties of the flight system) it is no surprise that the close relationship between f_{max} and *WBF* has evolved. IFI-3a *WBF* was reduced compared to IFI *WBF*, corresponding to the slower IFI-3a f_{max}. This reduction in *WBF* should benefit IFI-3a *Drosophila* because IFI-3a flies can extract 33% more power from their flight muscles at the lower *WBF* of 129 Hz than if they beat their wings at 148 Hz, the *WBF* of IFI flies.

There is probably both a voluntary and involuntary component of the decrease in *WBF*. Currently it is believed that wing beat frequency is set by the inertia of the wings and stiffness of the flight system, including cuticle and flight musculature (Dickinson et al., 1997). Flies can voluntarily alter *WBF* over a limited range (e.g., *WBF* is increased to gain elevation) by modulating the stiffness of the flight system through the innervation of the direct flight muscle (Lehmann and Dickinson, 1997). Thus, IFI-3a flies might actively decrease *WBF* to enable higher power generation from its flight muscles via the same modulatory mechanism.

Alternatively, or in addition, the reduced stiffness of IFI-3a fibers compared to IFI fibers (elastic modulus) could be forcing the observed decrease in *WBF*. Molloy et al. (1993) modeled *WBF* of flies using a ''tuning fork'' equation: $WBF = (1/2\pi)\sqrt{k_m/I}$, where k_m = muscle stiffness and I = moment of inertia of the wings. Given $k_m = 267$ and 343 Nm^{-3} for IFI-3a and IFI, respectively (the elastic modulus amplitude values at 150 Hz), we predict that the

WBF of IFI-3a is 88% of IFI (assuming no change in moment of inertia), yielding a predicted *WBF* for IFI-3a flies of 130 Hz, given the observed *WBF* mean (148 Hz) for IFI flies at 15°C. The predicted decrease is consistent with the observed 129 Hz *WBF* at 15°C for IFI-3a flies, suggesting that the reduction is primarily an involuntary action.

Regardless of the mechanism, the observed decrease in *WBF* sacrifices aerodynamic power ($P_{aero} \sim WBF^3$), especially at 15°C. The decrease in temperature had equal effects on IFI and IFI-3a *WBF*, as in both cases *WBF* dropped to 78% of their respective *WBF*s at room temperature. However, the drop of IFI-3a *WBF* to 129 Hz severely decreases flight ability as IFI-3a flight index decreases to 1.5, whereas IFI flight index remains at 4 for a *WBF* of 148 Hz (Table 4). Assuming there is no other compounding effect of temperature on aerodynamic power besides the *WBF* decrease, the difference in flight index between IFI-3a and IFI suggests that a *WBF* of ~129 Hz is borderline for flight. However, it is remarkable that *Drosophila* can fly at all when its flight muscle is expressing myosin with dramatically different molecular properties from the native isoform. Surely this is a testament to the amazing adaptability of the organism and muscle.

REFERENCES

Babu, G. J., E. Loukianov, T. Loukianova, G. J. Pyne, S. Huke, G. Osol, R. B. Low, R. J. Paul, and M. Periasamy. 2001. Loss of SM-B myosin affects muscle shortening velocity and maximal force development. *Nat. Cell Biol.* 3:1025–1029.

Bernstein, S. I., and R. A. Milligan. 1997. Fine tuning a molecular motor: the location of alternative domains in the *Drosophila* myosin head. *J. Mol. Biol.* 271:1–6.

Bernstein, S. I., K. Mogami, J. J. Donady, and C. P. Emerson, Jr. 1983. *Drosophila* muscle myosin heavy chain encoded by a single gene in a cluster of muscle mutations. *Nature.* 302:393–397.

Blanchard, E. M., K. Iizuka, M. Christe, D. A. Conner, A. Geisterfer-Lowrance, F. J. Schoen, D. W. Maughan, C. E. Seidman, and J. G. Seidman. 1997. Targeted ablation of the murine alpha-tropomyosin gene. *Circ. Res.* 81:1005–1010.

Burghardt, T. P., A. R. Cruz-Walker, S. Park, and K. Ajtai. 2001. Conformation of myosin interdomain interactions during contraction: deductions from muscle fibers using polarized fluorescence. *Biochemistry.* 40:4821–4833.

Cripps, R. M., and S. I. Bernstein. 2000. Generation of transgenic *Drosophila melanogaster* by *P* element-mediated germline transformation. *In* Introducing DNA into Living Cells and Organisms. P. A. Norton and L. F. Steel, editors. BioTechniques Books, Eaton Publishing, Natick, MA.

Dickinson, M. H., C. J. Hyatt, F.-O. Lehmann, J. R. Moore, M. C. Reedy, A. Simcox, R. Tohtong, J. O. Vigoreaux, H. Yamashita, and D. W. Maughan. 1997. Phosphorylation-dependent power output of transgenic flies: an integrated study. *Biophys. J.* 73:3122–3134.

Drummond, D. R., M. Peckham, J. C. Sparrow, and D. C. S. White. 1990. Alteration in crossbridge kinetics caused by mutations in actin. *Nature.* 348:440–442.

Ford, L. E., A. F. Huxley, and R. M. Simmons. 1977. Tension responses to sudden length change in stimulated frog muscle fibres near slack length. *J. Physiol.* 269:441–515.

Geeves, M. A. 1991. The dynamics of actin and myosin association and the crossbridge model of muscle contraction. *Biochem. J.* 274:1–14.

George, E. L., M. B. Ober, and C. P. Emerson. 1989. Functional domains of the *Drosophila melanogaster* muscle myosin heavy-chain are encoded by alternatively spliced exons. *Mol. Cell. Biol.* 9:2957–2974.

Hastings, K. E., and C. P. Emerson, Jr. 1982. cDNA clone analysis of six co-regulated mRNAs encoding skeletal muscle contractile proteins. *Proc. Natl. Acad. Sci. USA.* 79:1553–1557.

Hyatt, C. J., and D. W. Maughan. 1994. Fourier analysis of wing beat signals: assessing the effects of genetic alterations of flight muscle structure in Diptera. *Biophys. J.* 67:1149–1154.

Kawai, M., and P. W. Brandt. 1980. Sinusoidal analysis: a high resolution method for correlating biochemical reactions with physiological processes in activated skeletal muscles of rabbit, frog and crayfish. *J. Muscle Res. Cell Motil.* 1:279–303.

Kovacs, M., A. Malnasi-Csizmadia, R. J. Woolley, and C. R. Bagshaw. 2002. Analysis of nucleotide binding to *Dictyostelium* myosin II motor domains containing a single tryptophan near the active site. *J. Biol. Chem.* 277:28459–28467.

Laurie-Ahlberg, C. C., P. T. Barnes, J. W. Curtsinger, T. H. Emigh, B. Karlin, R. Morris, R. A. Norman, and A. N. Wilton. 1985. Genetic variability of flight muscle metabolism in *Drosophila melanogaster.* II. Relationship between power output and enzyme activity levels. *Genetics.* 111:845–868.

Lehmann, F. O., and M. H. Dickinson. 1997. The changes in power requirements and muscle efficiency during elevated flight force production in the fruit fly, *Drosophila. J. Exp. Biol.* 200:1133–1143.

Littlefield, K. P., D. M. Swank, B. M. Sanchez, A. F. Knowles, D. M. Warshaw, and S. I. Bernstein. 2003. The converter domain modulates kinetic properties of *Drosophila* myosin. *Am. J. Physiol.* 284:C1031–C1038.

Lowey, S., G. S. Waller, and K. M. Trybus. 1993. Function of skeletal muscle myosin heavy and light chain isoforms by an *in vitro* motility assay. *J. Biol. Chem.* 268:20414–20418.

Maughan, D. W., and J. O. Vigoreaux. 1999. An integrated view of insect flight muscle: genes, motor molecules, and motion. *News Physiol. Sci.* 14:87–92.

Molloy, J., A. Kreuz, R. Miller, T. Tansey, and D. Maughan. 1993. Effects of tropomyosin deficiency in flight muscle of *Drosophila melanogaster.* *In* Mechanism of Myofilament Sliding in Muscle Contraction. H. Sugi and G. H. Pollack, editors. Plenum Press, New York, NY. 165–172.

Molloy, J. E., V. Kyrtatas, J. C. Sparrow, and D. C. S. White. 1987. Kinetics of flight muscles from insects with different wing beat frequencies. *Nature.* 328:429–451.

Mulieri, L. A., W. Barnes, B. J. Leavitt, F. P. Ittleman, M. M. LeWinter, N. R. Alpert, and D. W. Maughan. 2002. Alterations of myocardial dynamic stiffness implicating abnormal crossbridge function in human mitral regurgitation heart failure. *Circ. Res.* 90:66–72.

Murphy, C. T., and J. A. Spudich. 2000. Variable surface loops and myosin activity: accessories to a motor. *J. Muscle Res. Cell Motil.* 21:139–151.

O'Donnell, P. T., and S. I. Bernstein. 1988. Molecular and ultrastructural defects in a *Drosophila* myosin heavy chain mutant: differential effects on muscle function produced by similar thick filament abnormalities. *J. Cell Biol.* 107:2601–2612.

Peckham, M., J. E. Molloy, J. C. Sparrow, and D. C. S. White. 1990. Physiological properties of the dorsal longitudinal flight muscle and the tergal depressor of the trochanter muscle of *Drosophila melanogaster.* *J. Muscle Res. Cell Motil.* 11:203–215.

Reedy, M. C., and C. Beall. 1993. Ultrastructure of developing flight muscle in *Drosophila.* I. Assembly of myofibrils. *Dev. Biol.* 160:443–465.

Rozek, C. E., and N. Davidson. 1983. *Drosophila* has one myosin heavy-chain gene with three developmentally regulated transcripts. *Cell.* 32:23–34.

Spudich, J. A. 1994. How molecular motors work. *Nature.* 372:515–518.

Steiger, G. J. 1977. Stretch activation and tension transients in cardiac, skeletal and insect flight muscle. *In* Insect Flight Muscle. R. T. Tregear, editor. North Holland, Amsterdam, The Netherlands. 221–268.

Swank, D. M., M. L. Bartoo, A. F. Knowles, C. Iliffe, S. I. Bernstein, J. E. Molloy, and J. C. Sparrow. 2001. Alternative exon-encoded regions of *Drosophila* myosin heavy chain modulate ATPase rates and actin sliding velocity. *J. Biol. Chem.* 276:15117–15124.

Swank, D. M., A. F. Knowles, W. A. Kronert, J. A. Suggs, G. E. Morrill, M. Nikkhoy, G. G. Manipon, and S. I. Bernstein. 2003. Variable N-terminal regions of muscle myosin heavy chain modulate ATPase rate and actin sliding velocity. *J. Biol. Chem.* 278:17475–17482.

Swank, D. M., A. F. Knowles, J. A. Suggs, F. Sarsoza, A. Lee, D. W. Maughan, and S. I. Bernstein. 2002. The myosin converter domain modulates muscle performance. *Nat. Cell Biol.* 4:312–317.

Swank, D. M., L. Wells, W. A. Kronert, G. E. Morrill, and S. I. Bernstein. 2000. Determining structure/function relationships for sarcomeric myosin heavy chain by genetic and transgenic manipulation of *Drosophila. Microsc. Res. Tech.* 50:430–442.

Tohtong, R., H. Yamashita, M. Graham, J. Haeberle, A. Simcox, and D. Maughan. 1995. Impairment of muscle function caused by mutations of phosphorylation sites in myosin regulatory light chain. *Nature.* 374:650–653.

Wells, L., K. A. Edwards, and S. I. Bernstein. 1996. Myosin heavy chain isoforms regulate muscle function but not myofibril assembly. *EMBO J.* 15:4454–4459.

Zhang, S., and S. I. Bernstein. 2001. Spatially and temporally regulated expression of myosin heavy chain alternative exons during *Drosophila* embryogenesis. *Mech. Dev.* 101:35–45.